

Supporting information

Low-temperature sprayed carbon electrode in modular HTL-free perovskite solar cells: comparative study on the choice of carbon sources

Ransheng Chen,^a Yulin Feng,^{ab} Jing Liu,^a Minhuan Wang,^a Hongru Ma,^b

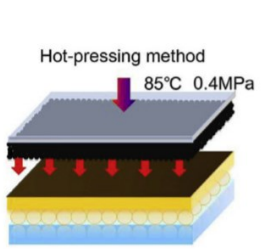
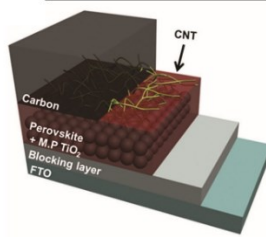
Jiming Bian*^a and Yantao Shi*^b

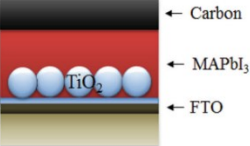
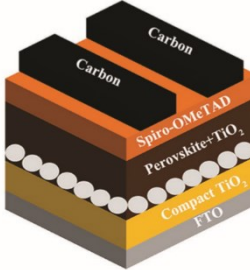
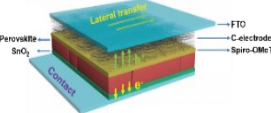
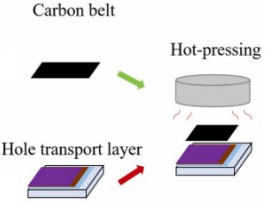
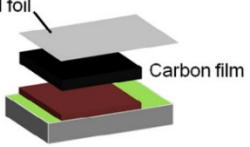
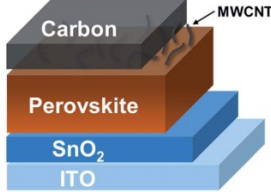
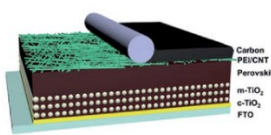
^a Key Laboratory of Materials Modification by Laser, Ion and Electron Beams (Ministry of Education), School of Physics, Dalian University of Technology, Dalian 116024, China

^b State Key Laboratory of Fine Chemicals, School of Chemistry, Dalian University of Technology, Dalian 116024, China

*Corresponding authors (emails: jmbian@dlut.edu.cn (Bian J); emails: shiyantao@dlut.edu.cn (Shi Y))

Table S1. A summary of device structure and photovoltaic performance of C-PSCs.

| Carbon-electrode PSCs Structure | Perovskite | Cell Area (cm ²) | V _{oc} (V) | J _{sc} (mA cm ⁻²) | PCE (%) | Ref. |
|---|--|------------------------------|---------------------|--|---------|------|
|  <p>Hot-pressing method 85°C 0.4MPa</p> | Cs _{0.05} (MA _{0.17} FA _{0.83}) _{0.95} Pb(I _{0.83} Br _{0.17}) ₃ | 0.30 | 0.89 | 22.29 | 10.84 | 11 |
| | | 1.00 | 0.84 | 22.39 | 8.72 | |
|  <p>Carbon CNT Perovskite + M.P.TiO₂ Blocking layer FTO</p> | Cs _{0.06} (MA _{0.17} FA _{0.83}) _{0.94} Pb(I _{0.84} Br _{0.16}) ₃ | 0.12 | 0.96 | 18.66 | 13.57 | 48 |
| | | 1.00 | 0.99 | 17.57 | 8.18 | |

| | | | | | | |
|---|--|----------------------|----------------------|------------------------|-----------------------|-----------|
|  | <p>MAPbI₃</p> | <p>0.07 1.00</p> | <p>1.04 0.99</p> | <p>21.27 19.63</p> | <p>14.38 9.72</p> | <p>40</p> |
|  | <p>FA_xMA_{1-x} PbI_yBr_{3-y}</p> | <p>0.1</p> | <p>1.08</p> | <p>23.33</p> | <p>19.2</p> | <p>16</p> |
|  | <p>Cs_{0.05}(FA_{0.85}MA_{0.15})_{0.95}Pb(I_{0.85}Br_{0.15})₃</p> | <p>1.30</p> | <p>1.05</p> | <p>22.78</p> | <p>18.65</p> | <p>35</p> |
|  | <p>CsFA_{0.83}MA_{0.17}PbI_{2.53}Br_{0.47}</p> | <p>0.115</p> | <p>1.09</p> | <p>21.1</p> | <p>15.3</p> | <p>32</p> |
|  | <p>CH₃NH₃PbI₃</p> | <p>0.08</p> | <p>1.002</p> | <p>21.30</p> | <p>13.53</p> | <p>25</p> |
|  | <p>FA_xMA_{1-x} PbI_yBr_{3-y}</p> | <p>1.0</p> | <p>1.01</p> | <p>20.48</p> | <p>12.34</p> | <p>34</p> |
|  | <p>CsPbI₃</p> | <p>0.08</p> | <p>0.80</p> | <p>18.58</p> | <p>10.55</p> | <p>50</p> |

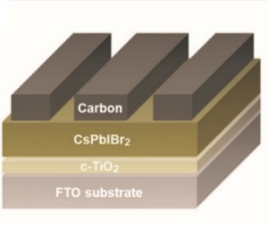
| | | | | | | |
|---|--------------------|------|-------|-------|------|----|
|  | CsPbIBr_2 | 0.09 | 1.245 | 10.66 | 9.16 | 33 |
|---|--------------------|------|-------|-------|------|----|

Table S2. Parameters of the TRPL spectroscopy based on the pristine perovskite films and perovskite/carbon sample with various carbon sources.

$$Y(t) = A_1 e^{-t/\tau_1} + A_2 e^{-t/\tau_2} + y_0 \quad *$$

MERGEFORMAT (1)

$$\tau_{ave} = \frac{A_1 \tau_1}{A_1 \tau_1 + A_2 \tau_2} \tau_1 + \frac{A_2 \tau_2}{A_1 \tau_1 + A_2 \tau_2} \tau_2 \quad *$$

MERGEFORMAT (2)

| Sample | τ_1 (ns) | Standard error | τ_2 (ns) | Standard error | τ_{ave} (ns) |
|------------|---------------|----------------|---------------|----------------|-------------------|
| Perovskite | 25.94 | 0.89 | 437.97 | 11.55 | 254.91 |
| MWCNT | 4.94 | 0.17 | 43.65 | 0.83 | 21.65 |
| Graphene | 3.64 | 0.12 | 68.98 | 1.36 | 29.28 |
| CNC | 15.35 | 0.83 | 133.66 | 9.56 | 51.77 |

Table S3. Parameters of the ultraviolet photoelectron spectra based on different carbon sources.

$$\phi = 21.2 - E_{cutoff} + E_{Fermi} \quad *$$

MERGEFORMAT (3)

| Carbon Sources | E_{cutoff} (eV) | E_{Fermi} (eV) | Work function (eV) |
|----------------|----------------------|---------------------|-----------------------|
| CNT | 16.67 | 0.49 | 5.02 |
| CNC | 16.72 | 1.65 | 6.13 |
| Graphene | 16.75 | 0.69 | 5.14 |

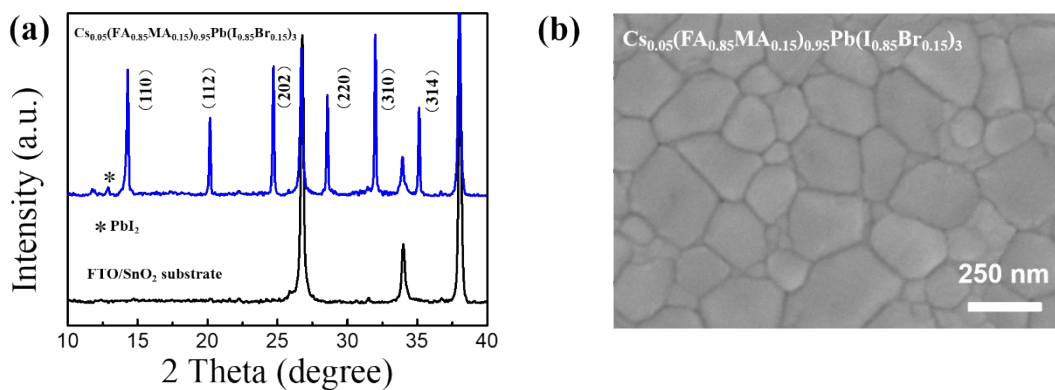


Fig. S1. (a) XRD patterns of the as-grown perovskite films. (b) top-view SEM images of perovskite films.

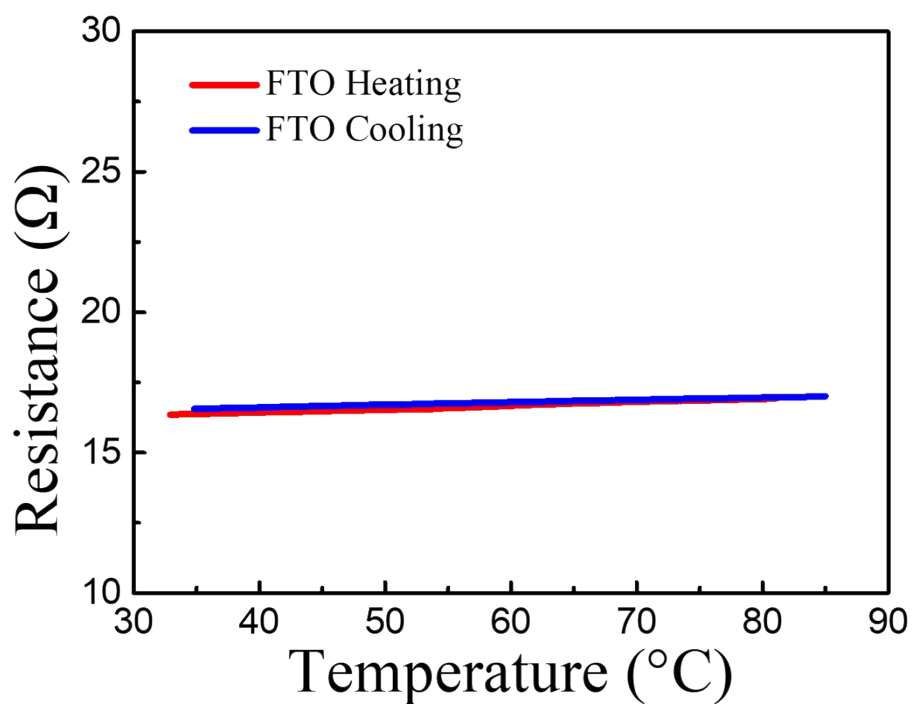


Fig. S2. The resistance- temperature curves of FTO film under heating and cooling process.

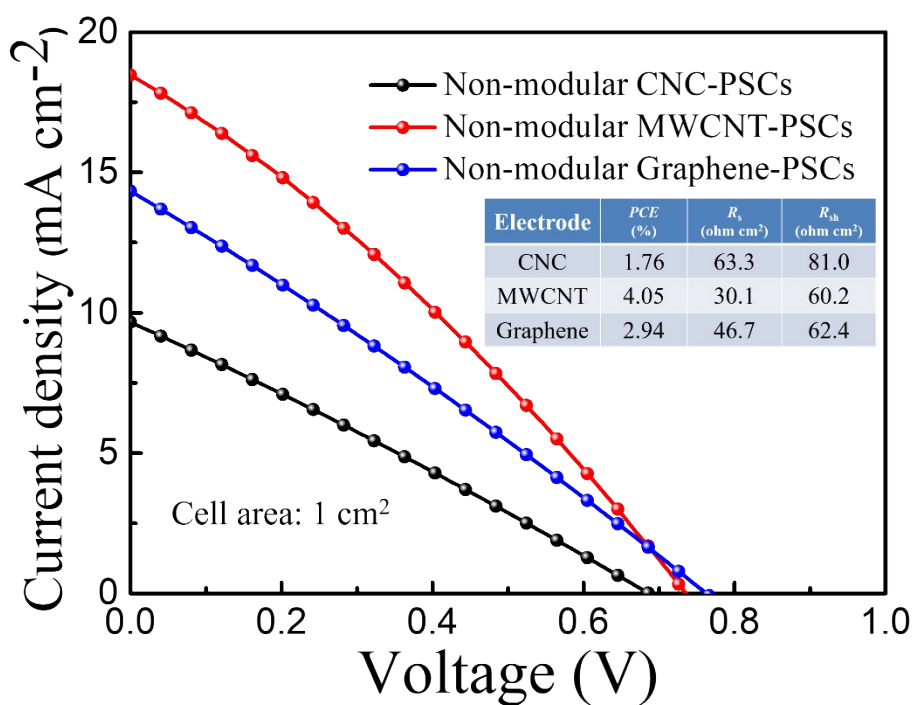


Fig. S3. J-V curves (cell area: 1 cm²) under solar simulator AM 1.5 of different carbon-based non-modular PSCs (CNC, MWCNT, Graphene).

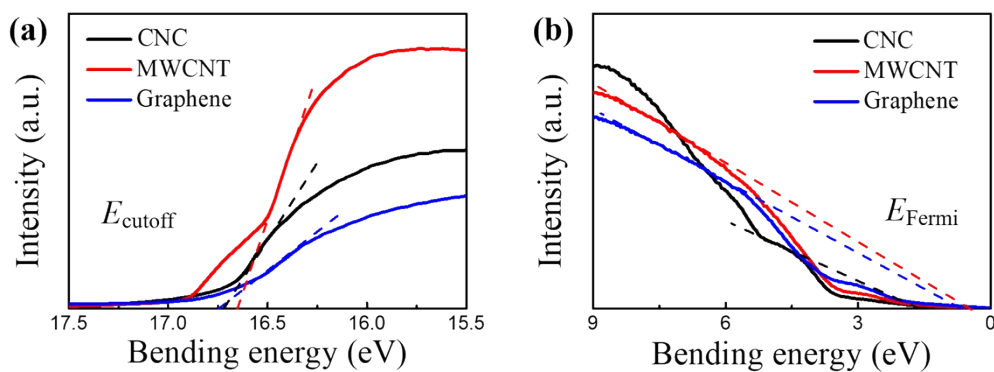


Fig. S4. (a) the cut-off energy (left part of Fig.4c) and (b) Fermi edge (right part of Fig.4c)

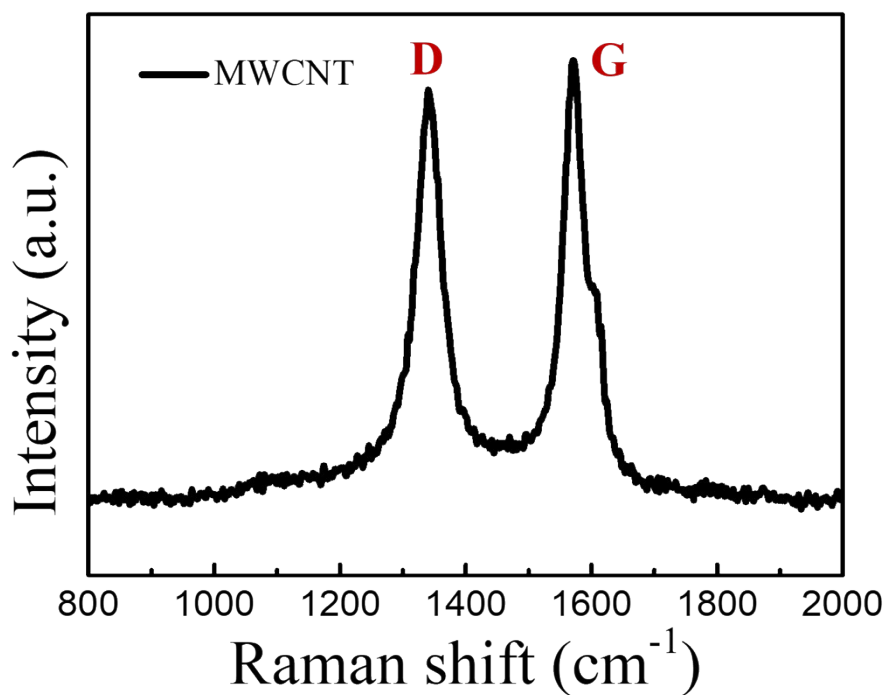


Fig. S5. Raman spectra of MWCNT, where the D-band originated from structural defects in carbon materials; the other G-band originated from graphite structure.

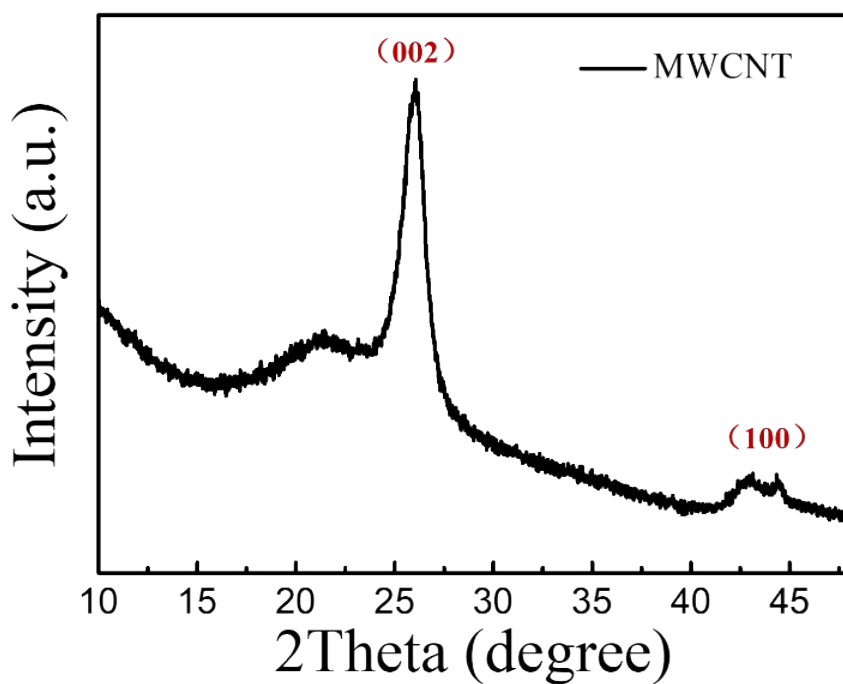


Fig. S6. XRD spectra of MWCNT.

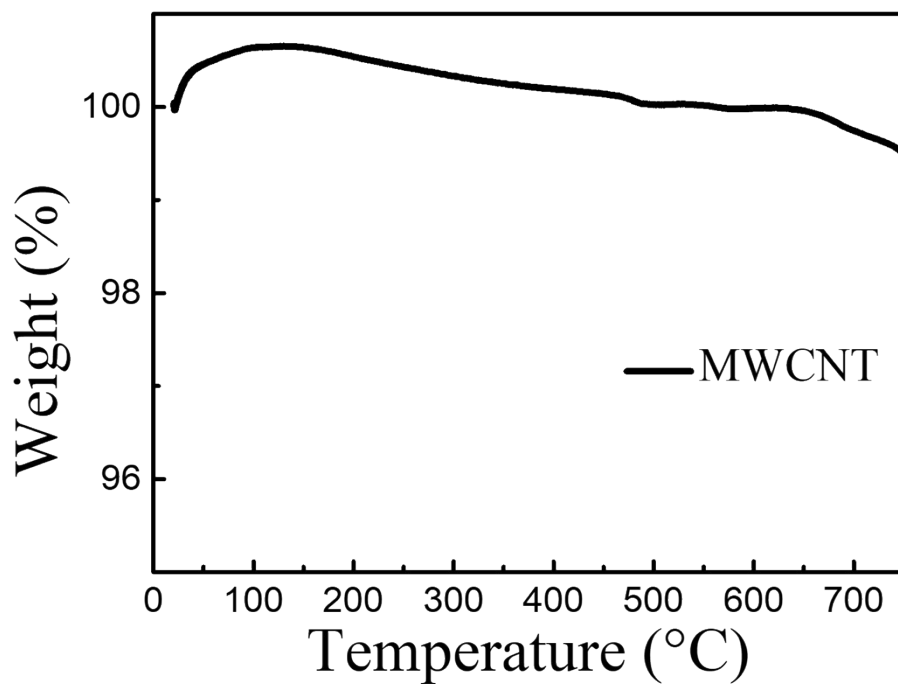


Fig. S7. Thermo gravimetric analysis (TGA) plot of MWCNT, which a convinced sign of thermal stability in the range of 25-800 °C.

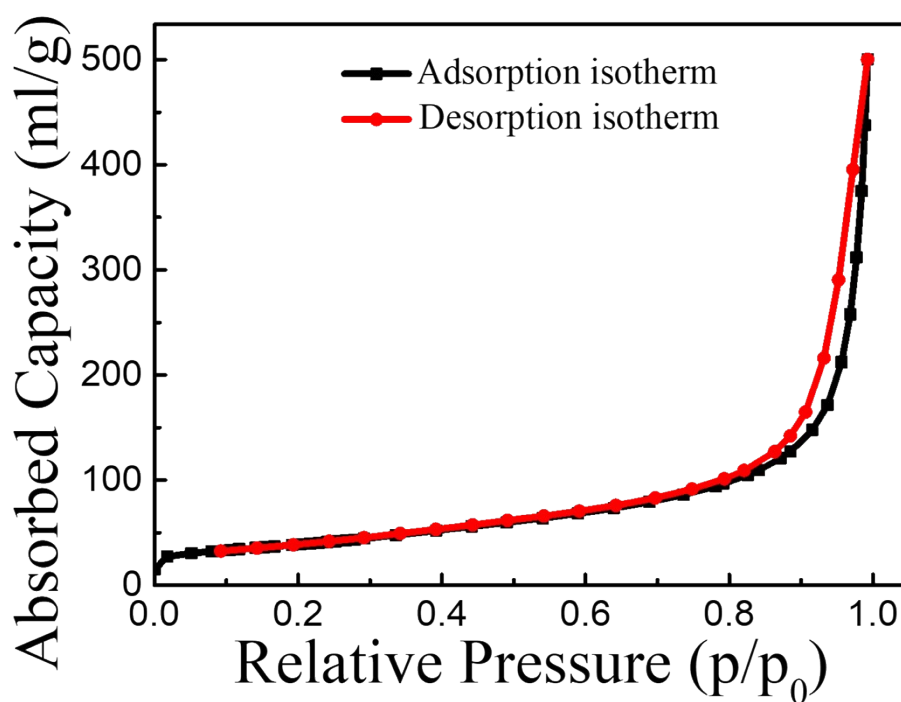


Fig. S8. Isotherm linear plot of MWCNT, and the specific surface area was 138.56 m²/g.

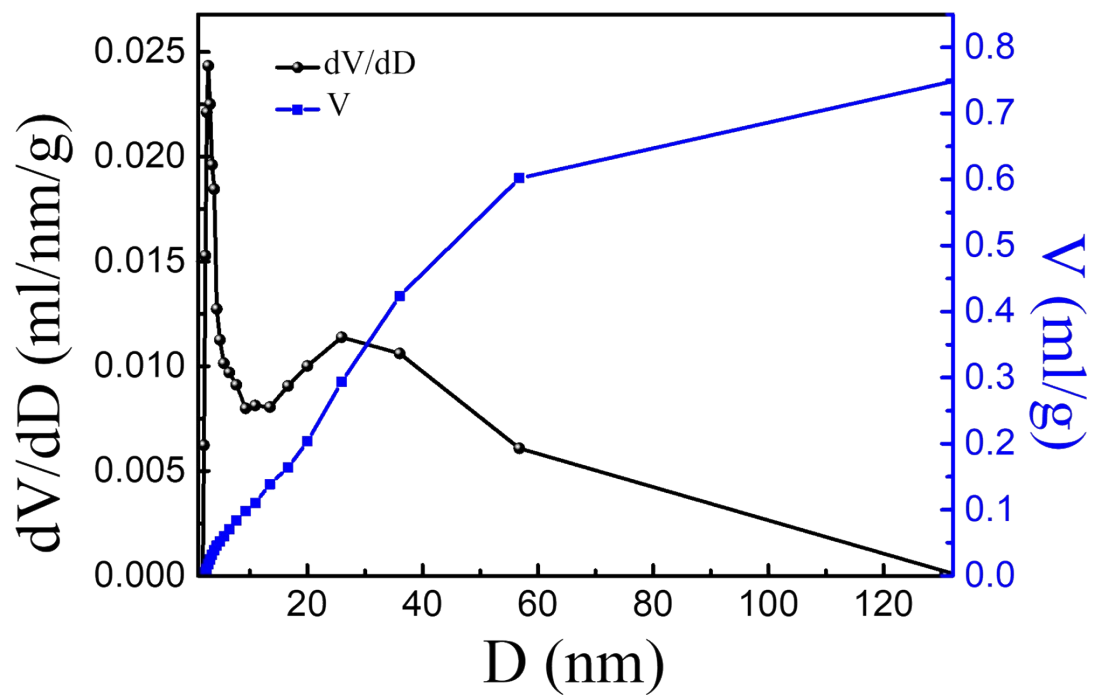


Fig. S9. Barrett-Joyner-Halenda (BJH desorption) pore volume & pore size curve of MWCNT, where the pore volume was 0.75 ml/g, the pore size was 16.31 nm.